Optimal Incorporation of Non-Traditional Sensors into the Space Domain Awareness Architecture

Albert R. Vasso
Air Force Institute of Technology (AFIT), Wright-Patterson AFB Ohio
Richard G. Cobb
AFIT, Wright-Patterson AFB Ohio
John M. Colombi
AFIT, Wright-Patterson AFB Ohio
Bryan D. Little
AFIT, Wright-Patterson AFB Ohio
David W. Meyer
AFIT, Wright-Patterson AFB Ohio

ABSTRACT

Space Domain Awareness (SDA) requirements are increasing while the United States Government (USG), the world's largest provider of SDA and Space Traffic Management (STM) services, struggles to update legacy hardware and address new threats. Recent policy asserts the need to utilize non-traditional sources to improve these mission areas, but no study has approached the problem as the optimization of a new, augmented USG/non-traditional network (AN). This multi-disciplinary study explores the problem by employing system architecting, physics-based modeling, optimization, and data analysis to resolve a hypothetical System Program Office (SPO) contracting decision. The SPO is charged with designing the AN, which is composed of the three Ground-Based Electro-Optical Deep Space Surveillance (GEODSS) systems, one contributing civil telescope, one contributing large allied scientific telescope, and some number of fully-taskable commercial small telescopes. The SPO must decide which of the 56 worldwide commercial sensors to purchase from three companies given a total cost constraint of $25M. Literature review and market research determined representative non-traditional capabilities while system architecting identified coverage, average capacity, and average latency to be amongst the most important measures of AN performance. A large-scale tradestudy exploring the 10^{16} possible AN architectures was conducted by modeling architectures and 954 Geosynchronous Earth Orbit (GEO) Resident Space Objects (RSOs) in Systems Tool Kit (STK) and custom Python scripts, then simulating architecture performance over a 24-hour collection period during Summer Solstice. The Non-Sorted Genetic Algorithm II (NSGA-II) heuristic method was used with Multi-Objective Optimization on five trials to advance 25,000 architectures and identify those with maximal coverage, maximal average capacity, and minimal average latency. 17 architectural choices were identified and, after analysis, five distinct AN design options were presented to the SPO's decision-maker based on a balance of capability and managerial factors. The methodology lays a foundation for assessing future AN options given a set of desirable measures.

1. INTRODUCTION

Reliance on space services is paramount for defense, civil, and commercial purposes. Space usage and debris concerns are projected to grow as responsive launches and improvements in technology lower barriers to space access; world actors solidify national space goals; and US policy pushes space-related objectives. The need to maintain Space Domain Awareness (SDA), specifically the tracking and cataloging of Resident Space Objects (RSOs), will clearly increase. Currently, the United States Government (USG) provides the world's de facto SDA and Space Traffic Management (STM) services through the data gleaned from a worldwide network of USG and allied radars, telescopes, and satellites. However, the USG will be hard-pressed to maintain SDA services in the future due to both the increased number of new RSOs and a failure to modernize equipment and processes.

Fortunately, recent technological advancements and the realization of business cases have prompted commercial entities to field their own SDA tracking networks. The USG recognizes that sensors from commercial, civil, and scientific organizations conducting related space missions may bring value to the SDA mission, and has publicly

outlined how it will vet non-traditional sensor providers for incorporation into the SDA pipeline. However, no framework for assessing the performance of the hybrid USG/non-traditional SDA architecture has been developed.

In this paper, amalgamating non-traditional capabilities represents the first step in addressing this problem. System needs and requirements for the hybrid architecture, henceforth referred to as the Augmented Network (AN), are then developed to garner desirable capabilities. Several key measures are then derived to quantify performance. These measures roughly capture coverage, the number of unique RSOs detected; capacity, the average number of observations on each RSO; and latency, the average maximum time between successive observations on each RSO. A model and simulation (M&S) of various AN architectures in the collection of RSOs over a 24-hour interval is conducted, from which the performance measures are tabulated. The large number of potential architectures, which is over 10^{16}, is such that Multi-Objective Optimization (MOO) using a heuristic method must be employed to identify a final list of several dozen high-performers. Data analysis then empowers a decision-maker to construct an AN architecture based on their personally-desired balance of capabilities, cost, and managerial factors.

Herein, a notional scenario is assumed to guide the development of the problem. A USG SDA System Program Office (SPO) is allocated $25M to incorporate Deep Space (DS) metric data from commercial, civil, and scientific providers directly into the SDA data framework. This number is based on a proposed 10% increase to the 2016 Government Accountability Office (GAO) estimate of the Air Force Space Command (AFSPC) Fiscal Year 2020 budget for new sensors and systems [1]. The SPO is unable to purchase all data from all commercial providers, and decides it will purchase a number of small-aperture, Narrow Field of View (NFOV), fully-taskable sensors from up to three companies in order to maintain operational control (OPCON) over processes. This permits USG to task and schedule its DoD-owned sensors with up to 56 additional commercial telescopes. Civil and scientific data is contributed at no-cost, but with no ability to influence the tasking. The sole US civil asset, the Meter-Class Autonomous Telescope (MCAT), contributes observations primarily on debris RSOs while the sole allied scientific asset, Brazil-Internacional Gigante Global Observatorio (BIGGO), contributes only serendipitous observations as seen in its large aperture Wide Field of View (WFOV) staring array. The SPO must decide how to construct the optimal AN architecture meeting the cost constraint of $25M by the proper selection of commercial sensors while accounting for the capabilities of the non-commercial sensors. Armed with the knowledge of system architecting and optimization, the SPO sets out to provide its decision-maker with options by conducting an architectural optimization study based on the results of a large-scale M&S of the various AN permutations.

For this notional scenario, the following assumptions are levied to limit the scope of this problem. Only cataloging, or the collection of metric observations, of Geosynchronous Earth Orbit (GEO) Resident Space Objects (RSOs) using ground-based telescopes is considered. This is an appropriate reduction of the problem as the majority of non-governmental SDA is conducted using ground-based optical systems for DS[1] purposes[2], and quantifying the utility of characterization data is much more nebulous. Only the nine Ground-Based Electro-Optical Deep Space Surveillance (GEODSS) sensors are considered for USG cataloging[3]. GEODSS and MCAT capabilities are based on open-source information; BIGGO is a hypothetical construct. All commercial sensor locations, capabilities, and business cases are hypothesized based on artistic license influenced by open-source information. Although only a fictitious scenario is examined, it is anticipated that the methodology developed and applied herein are directly applicable to questions the USG is currently considering.

2. BACKGROUND

To understand the problem at hand, a review of the relevant disciplines is conducted. Current USG SDA techniques and processes are then detailed. Discussion of non-traditional SDA capabilities are then discussed.

REVIEW OF RELEVANT DISCIPLINES

System Architecting, Needs, and Decision-Making

Crawley et al. state that an architecture is "an abstract description of the entities of a system and the relationship between those entities…[which] can be represented as a set of decisions" [2]. Maier & Rechtin define the discipline of systems architecting as the art and science of creating and building complex systems through use of qualitative

[1] For the purposes of this study, DS RSOs are those with periods greater than 225 min not in cislunar trajectories.
[2] The radar capabilities for Low Earth Orbit (LEO) and occasional DS cataloging, as well Radio Frequency detection methods, are acknowledged as legitimate phenomenologies which are neglected for this study.
[3] Future work aspires to include Space Surveillance Telescope (SST) and space-based contributions.

heuristic principles and quantitative analytical techniques [3]. The system architect thus seeks to first loosely define a system's parameters, identify and prioritize trades, and evaluate alternatives based on desirable performance. Key to system architecting is the needs-to-goals framework, where needs are often expressed in ambiguous terms and consist of necessities, wants, and desires for improvements while goals are similar to high-level requirements and can be traded against other product and system attributes in the design phase [2].

Needs and requirements allow the system architect to define potential system architectures, while pre-defined measures assess performance. The discipline of decision analysis aids the evaluation of alternatives. While several decision analysis methods exist, a common approach employs Value-Focused Thinking [4]. Value-Focused thinking starts by considering decision-maker values and objectives prior to identifying alternatives. Next, gaps in valued objectives are qualitatively and quantitatively defined. Finally, decision opportunities are identified, and the values are used to evaluate alternatives. During the evaluation portion, a typical approach is to apply weights to all values and sum the results into an overall score. The selection of weights can be best performed by consulting with senior decision-makers and stakeholders, but is still subjective. An alternative approach employs optimization.

Optimization

Optimization may be defined as "a procedure of finding and comparing feasible solutions until no better solution can be found" [5]. Many real-world problems require a solution amongst competing goals which can be modeled and solved using MOO, in which multiple objective functions are minimized or maximized subject to constraints. Handling multiple objective functions poses the dilemma of how much to balance the minimization or maximization between the functions and how to compare final results. One technique to compare final results is to convert the problem into a scalar objective problem by weighting each objective, then summing the products such that

$$F(x) = w_1 f_1(x) + w_2 f_2(x) + \cdots + w_n f_n(x)$$
$$\sum_{1}^{n} w_n = 1 \tag{1.1}$$

This approach requires a perfect knowledge of the weights, since arbitrarily assumed values eliminate potential solutions. An alternative is to employ Pareto optimality. Fig. 1 illustrates this concept for a program with two objective functions being minimized, where each point on the curve is an optimal. Clearly, the best solution is the one at the origin or utopia point, but this point is generally infeasible. Optimals are ranked based on their ability to outperform, or be non-dominated by, other values. These rankings form fronts, where the set of non-dominated optimals closest to the utopia point form the Pareto Front and represent the best solutions to the problem.

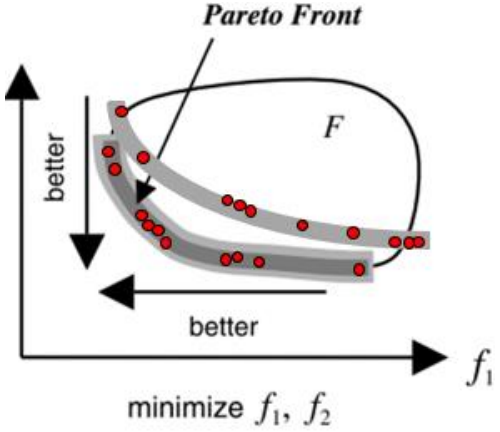

Fig. 1. Pareto Optimality [6]

In regards to the decision-making techniques discussed in the previous section, Crawley et al. recommends using MOO to evaluate a system's design tradespace, which includes "numerous architectures, represented at lower fidelity and evaluated with a few simple key metrics," and considering Pareto and near-Pareto optimal solutions for

exploitation [2]. Evaluation is expected to find clusters which suggest "families of architectures that achieve similar performance in one or more metrics".

NSGA-II

Evaluating optimization problems requires the use of search methods, which may be categorized as deterministic or stochastic. Stochastic methods are a better approach for large, complex tradespaces. A common stochastic method is the Non-Sorted Genetic Algorithm II (NSGA-II) [7]. First, an individual, or architecture for the problem at hand, is recast as a *gene* or *string* consisting of a number of *chromosomes*. Chromosome values are called *alleles*. A simple problem which aims to represent an architecture trade consisting of four sensor choices may be written as

$$\begin{gathered} a = s_1 s_2 s_3 s_4 \\ s_1 \dots s_4 = \{0,1\} \end{gathered} \tag{1.2}$$

An initial *parent* population of individuals is randomly selected. Each individual is evaluated based on the objective functions. All individuals are then ranked using non-dominated sorting; individuals on the same front are ranked higher when they are spaced farther apart from others. To identify best performers, a binary tournament randomly pits individuals against each other and advances the higher-ranked. The string representing each individual is spliced and exchanged with that of others in the crossover phase, creating *children*. Random mutations are also introduced such as a bit flip. The best individuals from the parent and children population are advanced to form the new population, which is used in the next *generation*. The process continues until all generations are evaluated.

Multiple *trials* of NSGA-II are typically conducted so as to fully explore the solution set. The choice of population size and the number of generations depend on the problem and researcher's prerogative. Haupt & Haupt assert that a Genetic Algorithm performing Pareto optimization needs a large population in order to define the Pareto Front [8]. Reeves mapped the minimum population size needed to solve a problem as a function of the length of the design chromosome and number of alleles per gene [9], while Harvey suggests a minimum size of 30 to 100 individuals based on experience [10]. Regarding the number of generations, researchers note that while more generations improve convergence, performing trial runs to identify diminishing returns may be most appropriate.

Optical Collection

The ultimate aim of fielding a space surveillance network is to perform Orbit Determination (OD) on the highest-quality data available, which is made possible by the following factors outlined by Vallado [11]. Geometric dispersion of observations such that multiple sensors obtain observations at different times, and collecting a large quantity of data, aids a better fit in OD routines. Employing multiple phenomenologies, improving sensor availability, and the tasking priority must also be considered. Ackermann et al. outline additional considerations which include weather at the site; cloud conditions; atmospheric visibility and stability; minimizing the amount of artificial sky brightness to improve discrimination on dim RSOs; and placing sites far enough from a populated area yet close enough for utilities [12].

Shell outlines an optical collection scenario in his paper[4] for monitoring orbital debris, stating the general process involves the optical system, the detector, the RSO, and the atmosphere and/or background [13]. Ultimately, the RSO's illumination must meet a certain Signal to Noise (SNR) threshold at the telescope's sensor array for a track to be considered successful. Howell defines the SNR for a Charged Coupled Device (CCD) as

$$SNR = \frac{e_s}{\sqrt{e_s + n_p(e_b + e_d + e_r^2)}} \tag{1.3}$$

where e_s is the total number of photoelectrons collected from the RSO, n_p is the number of pixels being considered, e_b is the total number of photoelectrons per pixel from the background or sky, e_d is the total number of dark current electrons per pixel, and e_r^2 is the total number of electrons per pixel resulting from read noise [14]. Typical thresholds for SNR success range from 2.5 to 6 depending on the techniques used and the observer's confidence in collection. The dark noise and read noise are properties of the sensor, while the number of pixels used in the calculation are set by the observer. The sky brightness may be empirically measured or estimated and consists of both ambient light and

[4] Unless otherwise stated, all equations are derived from Shell.

moonlight. Previous work by Thomas & Cobb has demonstrated radiance may be modeled using AFIT's high-fidelity Laser Environmental Effects Definition and Reference (LEEDR) routine [15].

The signal at the detector may be expressed as

$$e_s = \eta \tau_{opt} A \tau_{atm} E_{RSO} t_{sig} \tag{1.4}$$

where η is the sensor's quantum efficiency, τ_{opt} is the system's optical transmittance, A is the telescope's aperture (m), τ_{atm} is the atmospheric transmittance at the site, E_{RSO} is the irradiance of the RSO (photons/s-m^2), and t_{sig} is the signal integration time (s). For a typical silicon-based sensor operating at 625 nm, the irradiance is given by

$$E_{RSO} = 5.6x10^{10}10^{-0.4m_{RSO}} \tag{1.5}$$

in units of photos/s-m^2, where m_{RSO} is the RSO's visual magnitude (M_v). τ_{atm} may be modeled using high-fidelity software such as MODTRAN or LEEDR or estimated using empirical observations. τ_{atm} varies by elevation θ, and for a known zenith value $\tau_{atm,zen}$ may be approximated by

$$\tau_{atm} = \left(\tau_{atm,zen}\right)^{sec(\pi/2-\theta)} \tag{1.6}$$

If orbital information and the RSO's standard M_v at 1000 km altitude and 50% illumination, $m_{RSO,std}$, are known then M_v at the sensor may be approximated using Schmunk's adaptation of Matson's formula [16]

$$m_{RSO} = M_{RSO,std} + 5\log_{10}(|R|) - 15 - 2.5\log_{10}\left[\sin(\psi) + \left(\pi - \frac{\pi\psi}{180}\right)\cos(\psi)\right] \tag{1.7}$$

where R is the range to the RSO (km) and ψ is the sun-RSO-site or phase angle (rad). The maximum signal integration time may be approximated as the transit time through a single pixel on the detector such that

$$t_{sig,max} = \frac{x}{f\omega} \tag{1.8}$$

where x is the detector's pixel size (m), f is the focal length (m), and ω is the RSO's angular rate (rad/s). For an RSO in GEO traveling at 15 arcsec/s, $\omega = 7.3 \text{ x } 10^{-5}$ rad/s.

The background contribution e_b may be expressed as

$$e_b = \frac{\eta \tau_{opt} \pi L_b x^2 t_{int}}{1 + 4(f/d)^2} \tag{1.9}$$

where L_b is the background radiance (photons/s-m^2-sr), t_{int} is the integration time (s), and d is the telescope's aperture diameter (m). For a silicon-based sensor, the background radiance is calculated by

$$L_b = (5.6)10^{10}10^{-0.4M_b}\left(\frac{180}{\pi}\right)^2 3600^2 \tag{1.10}$$

where M_b is the background radiance at the site in units of M_v/arcsec^2. M_b may be empirically measured, approximated using high-fidelity software, or more simply modeled by combining brightness B in nanoLamberts (nL) for a clear moonless light with an approximation of the changing lunar brightness such that

$$B = B_{site,clearMoonless} + B_{lunar} \tag{1.11}$$

In their foundational model of lunar brightness Krisciunas & Schaefer [17] provide the relation between M_b and B as

$$M_b = \left(\frac{1}{0.92104}\right)\left[-ln\left(\frac{B}{34.08}\right) + 20.7233\right] \tag{1.12}$$

To first order, the brightness during umbra on a clear, moonless night may be assumed constant at a given elevation angle. Shell empirically derived the radiance at a site as a function of elevation and a known zenith quantity; on a clear moonless night this may be used to represented the brightness at the site by

$$B_{site,clearMoonless} = B_{site,clearMoonless,zen}(-0.6118\theta^3 + 2.6249\theta^2 - 3.8585\theta + 2.9482) \quad (1.13)$$

where values for $B_{site,clearMoonless,zen}$ are empirically derived and are typically around 19 to 21 in units of Mv/arcsec^2.

Krisciunas & Schaefer's model of lunar brightness uses various empirically-derived factors which fundamentally require knowledge of the atmospheric extinction coefficient k, sky position zenith angle ρ, the lunar phase angle α, the lunar zenith angle Z_m, and the RSO's zenith angle Z as measured from the site[5]. k is empirically derived or assumed; ρ is the angle formed by the site-moon and site-RSO vector; α is the angle formed by the sun-moon-earth geometry, and the zenith angle is computed by

$$Z = \frac{\pi}{2} - \theta \quad (1.14)$$

B_{lunar} is calculated using the Rayleigh Scattering function $f(\rho)$, the illuminance of the moon outside the atmosphere I^*, and the distance of the moon $X(Z)$ based on zenith angle such that

$$\begin{gathered} B_{moon} = f(\rho) I^* 10^{-0.4kX(Z_m)}\left[1 - 10^{-0.4kX(Z)}\right] \\ f(\rho) = 10^{5.36}[1.06 + cos^2(\rho)] + 10^{6.15-\frac{\rho}{40}} \\ I^* = 10^{-0.4(3.84+0.026|\alpha|+4\times10^{-9}\alpha^4)} \\ X(Z) = (1 - 0.96sin^2 Z)^{-0.5} \end{gathered} \quad (1.15)$$

Astrodynamics

OD is the process by which knowledge of an RSO's motion relative to the center of mass of the Earth is obtained [18]. Uncertainty is an important concept in OD problems. Due to limitations in sensor capabilities, approximations in equations and models, and measurement errors, the true state of an RSO is rarely known. The overall uncertainty of the state is represented by the RSO's *covariance*. OD begins as soon as observations are collected. In a sideral collection mode, a telescope watches for an RSO and a streak is generated. The streak is processed and both endpoints are used to get two observations [11]. A minimum of three observations are required to form a *tracklet* and compute an orbit [19]. The observations are roughly correlated to known RSOs in the catalog via Initial Orbit Determination [11].

When orbital parameters and uncertainty are known, physics-based models may be used to estimate an RSO's position forward or backward in time. From this predictive information, an RSO's future location may be projected, inferring behavior, capabilities, and the potential for a collision with another RSO. A common orbital propagation algorithm is Simplified General Perturbations 4 (SGP4), which uses analytical techniques to obtain approximate solutions by using a reference solution with a perturbation [18].

Scheduling

The 2004 edition of Strategic Command Document 505-1 (SD 505-1) Volume 2 states that for the "most accurate orbit determination, observations should be taken at different positions on a satellite's orbital path…ideally, cover[ing] the full 360 degrees of an orbit" but since this is unrealistic, sensor tasking and scheduling must be conducted [20]. The AFSPC Astrodynamics Innovation Committee (AIC) define this goal as "allocate[ing] resources appropriately in order to gain as much information as possible about a system…[and] optimiz[ing] system performance while simultaneously meeting as many, if not all, of the requirements as possible" [21]. The principal concern for SDA scheduling scenarios is collecting prioritized RSOs to a requisite capacity and/or geometric diversity, by particular sensors with finite access times and capability limitations, so that RSO covariance knowledge is minimized. There are several commonly-employed scheduling methods in the SDA academic and operational communities.

[5] Krisciunas & Schaefer use degrees instead of radians, which requires care when employing the angles in the non-trigonometric portions.

In rough order of increasing rigor and computational complexity are the Greedy algorithm; scheduling theory problems; and information gain routines. The Greedy algorithm prioritizes a list of RSOs and steps through all sensors by time, merely assigning the first RSO in the list to an observation. While fast, this method does not optimally place resources. A pure scheduling theory approach employs an optimization program to enforce collection constraints. These approaches employ integer programming which requires slower solver routines. Newer techniques include scheduling based on projecting which observations will best minimize covariance or maximize information gain.

Advanced techniques, however, do not necessarily equate to major performance gains. In his SDA collection scenario using an SD 505-1-derived Greedy scheduling routine and a binary integer program, Dararutana showed the integer program increased computation time by a factor of 10 while only increasing the number of unique RSOs collected by 2% [22]. Using an appropriate scheduling technique which capitalizes on the geometric diversity and frequent contributions of multiple sensors is key to realizing the AN's maximum utility.

CURRENT USG SDA PROCESSES

The USG uses a worldwide system of ground- and space-based telescopes and ground-based radars to perform SDA via the Space Surveillance Network (SSN). Sensors collect data which is collated and stored in a central database. Algorithms are then run on the data to develop information, which leads to tasking of sensors to improve knowledge. Finally, information is disseminated to various customers. The collection of cataloging data on DS RSOs is primarily performed using ground- and space-based optical platforms, although DS radars may also be utilized. Current optical cataloging sensors include the nine GEODSS sensors, three each in Socorro New Mexico, Maui Hawaii, and Diego Garcia; the Space Surveillance Telescope in Exmouth Australia; and the Space-Based Space Surveillance (SBSS), Operationally Responsive Space 5 (ORS-5), and Sapphire satellites.

The core of the SSN is the Space Defense Operations Center (SPADOC) and the Correlation, Analysis, and Verification of Ephemerides Network (CAVENet) systems. SPADOC and CAVENet are used to process observations on RSOs, maintain the catalog, perform conjunction assessments, and detect threats. SPADOC's limited processing power permits it to only perform calculations using general perturbation theory; additional work is conducted on CAVENet via its Astrodynamic Support Workstation (ASW). Observations flow from all sensors into the systems, and orbit determination is performed when a certain threshold of positional accuracy is met. Resultant products are state vectors and Two-Line Element Sets (TLEs, or ELSETs), the later using traditional Keplerian orbital parameters.

SDA has traditionally been a nation-state activity, and the US has historically been reluctant to disclose high-accuracy catalog information due to concerns its capabilities may be derived. The 2009 Iridium/Cosmos collision has been cited as the turning point in which providing limited conjunction assessment data was felt to outweigh OPSEC concerns [23]. The same year, USSTRATCOM instituted the SSA Sharing Program, allowing private citizens to receive basic orbit tracking data via Space-Track.org. Data from the high accuracy catalog, which is much more precise and includes state covariance information, is only available via special sharing agreement [24].

After the Iridium/Cosmos collision, the DoD began active coordination with RSO owners/operators to ensure greater community awareness of conjunction threats. The DoD has in effect become the world's major broker of basic space tracking data and unofficial coordinator for parties with conjunction concerns. This general process has been deemed Space Traffic Management (STM), defined as "the planning, coordination, and on-orbit synchronization of activities to enhance the safety, stability, and sustainability of operations in the space environment" [25]. In 2018, President Trump issued Space Policy Directive 3 (SPD-3), National Space Traffic Management Policy, which necessitates turning over the STM mission to the Department of Commerce (DoC). SPD-3 asserts the Secretary of Defense will maintain authority over the space catalog which implies the DoD will still conduct the foundational SDA mission while the majority of stakeholder engagement becomes the responsibility of DoC.

DoD breaks the sensor management problem into two parts: tasking and scheduling. DoD performs centralized tasking at the headquarters level, then decentralizes scheduling to the sensors. Tasking consists of assigning RSOs to be observed by one or more sensors, while scheduling is the time-based lineup of RSOs each sensor plans to collect. This process is employed instead of centralized tasking and centralized scheduling due to computational burdens on the centralized computer, the inability to control the tasking of contributing and collateral sensors, and the challenges of sensor-specific constraints [21], [26].

Once orbital parameters are available, astrodynamical software is used to propagate multiple RSOs into the future. The available information is used to determine when the RSO will likely be trackable again, which feeds into the next tracking cycle. DoD performs high accuracy catalog screenings in DS every 24 hours, and Near-Earth (NE) every eight hours. Ephemerides are calculated for high-interest screenings on demand, every 12 hours for DS RSOs, and every eight hours for NE RSOs [27]. Extrapolated General Perturbation ELSETs are taken from the high-accuracy catalog, stored as TLEs without covariance, and provided on Space-track.org. Lal asserts that "because they do not

have covariance, they may not be optimal for advanced analysis and risk assessment; however, they are accurate for fairly long periods of time" [27]. Limited covariance information is provided to registered owners/operators. STM efforts are also conducted as a public service for the world. Conjunction Assessments (CAs) are run to determine the probability of collisions between RSOs; if CAs exceed acceptable limits, 18 SPCS alerts owners/operators.

IMPETUS FOR CHANGE

The USG SDA mission is currently challenged by several factors. The volume of new RSOs in orbit, projected to be in orbit, and detectable by newer sensors is increasing due to a reduction in hardware costs, an increase in launch rates, and new business cases for space-based platforms. Coupled with the potential for more debris, this necessitates an increase in cataloging and conjunction assessments. New threats from foreign actors is also requiring increased and novel approaches to SDA. Lastly, the USG is unable to quickly improve mission execution due to reliance on legacy systems such as SPADOC which have computational limitations incompatible with future SDA needs.

The 2011 Technology Horizons study lists persistent SDA as a high-priority technology area which would be needed by 2030 [28]. The 2017 National Security Strategy calls upon renewing key capabilities in space to address global challenges, asserting that "the United States considers unfettered access to and freedom to operate in space to be a vital interest" [29]. The reactivation of the United States Space Command (USSPACECOM) and creation of the United States Space Force (USSF) attest to the growing importance of the space domain.

The publication of SPD-3 in 2018 represents the call to action for improving SDA and STM practices. The document asserts that "as the number of space objects increases…[the current] limited traffic management activity and architecture will become inadequate" and directs executive departments to pursue: improvements in observational data, algorithms, and models; developing new hardware and software to support data processing and observations; mitigating the effect of orbital debris; improving SDA data interoperability; and enabling greater data sharing. Agencies are also directed to improve SDA coverage and accuracy by seeking to minimize deficiencies in SDA capability, "particularly coverage in regions with limited sensor availability and sensitivity in detection of small debris" through data sharing, data purchase, or the provision of new sensors; developing better tracking capabilities; and developing the standards and protocols for creation of an open architecture data repository.

The 2019 AFSPC Instruction 10-610 (AFSPCI 10-610), SSA Metric Data Integration Guidelines for Non-Traditional Sensors[6], represents as response to SPD-3. It provides authoritative guidance on utilizing commercial SDA capabilities, stating that the "intent is to improve SDA through the utilization of a wide variety of sensor data and ephemeris data, of varying fidelity and accuracy, from an array of USG, non-DoD, commercial, civil and foreign data providers" while emphasizing that "the quality and compatibility criteria for new data sources should be set as broadly as possible". The research herein directly addresses this mandate.

COMMERCIAL AND SCIENTIFIC SDA CAPABILITIES

In 2018 Lal et al. researched global trends in SDA and STM while interviewing several commercial SDA stakeholders. They concluded that "due to perceptions related to lack of transparency with DoD data, and motivated by the desire for increasing self-reliance, some countries and companies either by themselves or through consortia are developing their own SSA catalogs" [27]. The ability to develop such catalogs for DS tracking has in part been spurred by improvements in optical sensing technology with a reduction in parts cost, permitting adequate telescopes for SDA to be purchased as Commercial Off the Shelf (COTS) items [27]. Because satellite owners/operators and governments value additional SDA data, multiple worldwide commercial networks rivaling DoD's coverage at the expense of lower fidelity now exist.

Three commercial companies conducting DS optical cataloging are Analytical Graphics Incorporated (AGI), ExoAnalytic Solutions, and the Numerica Corporation. In 2014, Oltrogge & Houlton outlined AGI's vision to "create a timely, accurate and complete [catalog] of space objects via [its] Commercial Space Operations Center (ComSpOC)…[using] a sensor network which is sufficiently diverse, both geographically and phenomenologically" and employs telescopes, radars, and radio telescopes with a focus on GEO RSO tracking [30]. Optical telescopes were placed to take advance of cloud-free locations in the southern hemisphere and southwestern US with an anticipated visual magnitude between 16-18 M_v and field of view (FOV) of 0.5°-1° for single telescope systems and 2π steradians for all-sky-staring optical systems.

ExoAnalytic has deployed its own worldwide telescope network consisting of over 230 sensors at 25 worldwide locations as of 2018 [31]. The company maintains a catalog of 2000 RSOs at altitudes greater than 10,000 km and

[6] As of writing, the document has not been re-released as a USSF regulation but is assumed authoritative.

claims to routinely achieve accuracies better than 0.25 arcsec in ideal conditions. ExoAnalytic posits that by combining observations from multiple sensors at one site, detection sensitivity as low as 21 M_v is routinely achieved. The company's public webpage provides an extensive list of services and prices. As of Feb 2020, two turn-key sensor packages are available: for $500K, one 14 in telescope with 1° FOV capable of observing RSOs down to 18.5 M_v with 0.2 arcsec accuracy, and for $5.5M, ten 14 in telescopes with 1° FOV capable of observing RSOs down to 20 M_v with 0.2 arcsec accuracy .

The Numerica Corporation network consists of "small-aperture, wide FOV sensors that provide persistent coverage of a large swath of the night sky, and medium-aperture telescopes that provide increased detectability and resolution but with a smaller FOV" [32]. Numerica has been working with the Air Force Research Laboratory (AFRL) to build a custom DS catalog with accuracy meeting or exceeding the DoD catalog; the majority of cataloged RSOs are in the 10-15 M_v brightness range. As of 2018, the network consisted of 15 sites across the world to provide 100% coverage of all DS orbital regimes. The telescopes were designed using COTS components along with custom-developed parts to provide robustness. 15 medium-aperture telescopes with 0.3-0.4 m performing rate tracking are augmented with 10 robotic sensor arrays conducting continuous collection of all RSOs in GEO or across swaths.

In 2018 Lal et al. indicated a "recent development has been the repurposing of existing sensors previously used for astronomy and other scientific research" [27]. Such sensors may be employed by the USG by accepting data on any or all RSOs they have collected, making agreements with sensor owners/operators to track particular RSOs at particular parts of the orbit, and by processing serendipitous data collected by the sensors. An example of scientific sensors whose data may be easily incorporated into the SSN are those used by the National Aeronautics and Space Administration (NASA) for orbital debris measurements [33]. NASA employs the 1.3 m MCAT telescope on Ascension Island to statistically characterize orbital debris at all altitudes and has advocated for its inclusion as a contributing sensor to the SSN [34].

Bellows demonstrated that ephemeris positional updates can be obtained using metric data from RSO streaks gathered serendipitously by astronomical telescopes which are observing other DS targets [35]. He cited the Panoramic Survey Telescope and Rapid Response System (Pan-STARRS) and the Large Synoptic Survey Telescope (LSST) as capable of providing advantages to DoD. This and similar work implies serendipitous data from other observatories may be utilized to improve the SDA mission; a cursory review has identified over 40 telescopes with a 3 m or greater aperture extant or in development, six of which are greater than 8 m [36], [37].

RELEVANT RESEARCH

The body of literature was reviewed and while no work directly addressing the problem posed herein was found, several related studies were identified. These may be loosely categorized as studies to augment the SSN with capabilities; studies to completely replace the SSN with a new network; and studies which delve into SDA requirement generation. The most pertinent augmentation studies are by Moomey and Raley. Moomey's 2015 work translated a Commander's Intent to improve SDA cataloging into the simulation of a worldwide network of small rate-tracking COTS telescopes through use of the systems engineering process [38]. By collecting on lower-priority bright RSOs, 60 telescopes at five sites were estimated to allow up to two hours of extra time per night on each GEODSS telescope. Raley summarized work conducted by the Defense Advanced Research Projects Agency (DARPA) OrbitOutlook program which demonstrated data from Space-Track.org and multiple civil, commercial, academic, and hobbyist providers could be combined to improve overall SDA goals while overcoming data surety concerns [39].

Noteworthy alternative SSN studies include Ackermann et al., Stern & Wachtel, Bateman, and Felten. Ackermann et al.'s 2015 work coupled modeling and simulation with expert knowledge of telescope siting constraints to design a network to outperform the SSN's DS tracking capabilities [40]. Stern & Wachtel sought to create an optimal network of SDA cataloging sensors from a large tradespace of ground and space-based telescopes by evaluating multiple architectures using MOO powered by a physics-based M&S of a nightly collection scenario [41]. Work by Bateman [42] and Felten [43] extended Stern & Wachtel's work with an improved methodology, M&S, and additional sensors. Stern & Wachtel's basic methodology is adopted in this work.

The last area of study concerns SDA requirements, which are needed to help understand likely AN requirements and evaluation measures. No open-source USG SDA nor SSN requirements document was found in literature, but Moomey's end-to-end system engineering approach with mission requirements and measures best illuminate the process and desired outcomes. Daw & Hejduk's 1999 study on SSN operational capabilities identified three target areas with associated measures: suitability, including accessibility and connectivity; effectiveness, including coverage, capacity, responsively, and detectability; and performance, including timeliness and quality. Lastly, AFSPCI 10-610 provides a good proxy to desirable AN measures via its Military Utility Assessment (MUA) criteria.

These include accuracy, capacity, sensitivity, field of regard/orbital coverage, search rate, tasking responsiveness, unique capabilities, availability, reliability, and cost.

3. METHODOLOGY

With the relevant disciplines reviewed, current processes outlined, need for change solidified, commercial capabilities covered, and related research addressed the methodology may now be outlined. This is depicted in Fig. 2. All portions will be reviewed except the scenario, which was covered to sufficient depth in the introduction.

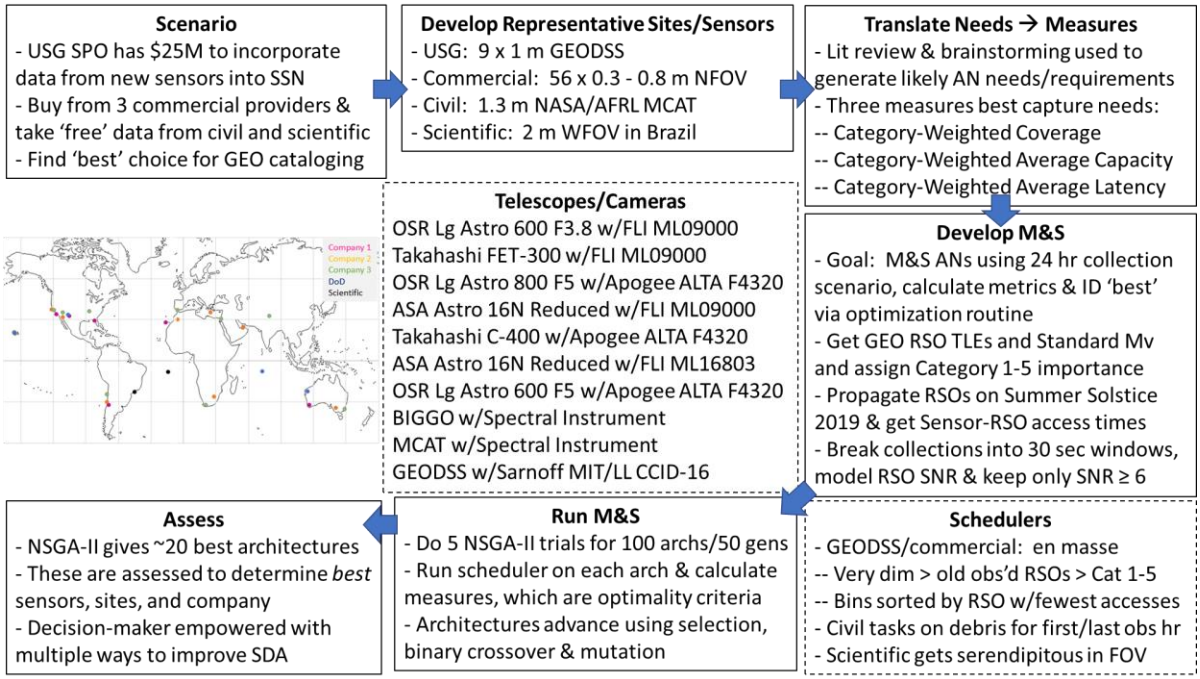

Figure 2. Methodology, where major steps are executed in a clockwise order. High-level detail on site locations, telescope/camera combinations, and scheduler information is also depicted.

DEVELOP REPRESENTATIVE SITES AND SENSORS

With one exception, only NFOV ground-based telescopes are considered. The telescopes are constrained to perform DS cataloging only using sidereal tracking.

DoD Sensors

The nine GEODSS telescopes form DoD's baseline network. Bruck & Copey [44] and Ackermann et al. [40] provide the majority of the telescope specifications. Each telescope is approximately 1 m in aperture with a 1.25° x 1.64° FOV.

Commercial Sensors

The references listed in the Commercial Capabilities section were used to elicit representative commercial sites and sensor parameters. The three major DS optical companies provide only coarse site latitude/longitude locations or names, which necessitates approximating locations. An assumption is made that providers deploy sensors at existing sites only. The prioritized deployment strategy was hypothesized to be at: large observatories with excellent viewing capabilities, smaller observatories in unique locations, and commercial or privately-operated remote telescope sites. With this prioritization in mind, each site's coarse latitude/longitude was matched to appropriate sites from a list of known observatories. The closest location is generally selected. On several occasions sites could not be immediately

matched until Internet searching revealed observatories not on the list. Google Maps was used to verify the latitude/longitude for the proposed sites. Sites which could not be matched to an observatory and which seemed to be used by multiple providers were dropped to reduce the problem space.

The three companies also provide information on their number of sensors and coarse capabilities. This in part includes: NFOV sensors on the order of 0.5° to 1°, 0.3-0.4 m apertures, and capabilities ranging between 10-15, 16-18, and 18.5 to 20 M_v. North's formulation of the telescope limiting magnitude estimation equation [45]

$$M_{v,lim} = 4.5 + 4.4 \log_{10}(d) \tag{1.16}$$

where d is the telescope diameter in mm indicates an approximately 1 m aperture is required to resolve RSOs of 18 M_v. Since the SDA community generally regards small telescopes to be below 1 m diameter, and larger telescopes cost more to design and deploy, this is felt to be an appropriate cutoff. Sensor costs are estimated to be at least $0.5M based on price data published by ExoAnalytic. Variations in pricing as well as likely additional cost to accommodate unique USG requirements are accounted for in the scenario.

With a list of known sites by providers, likely capabilities, and potential costs the sites were shuffled amongst the providers and sensors allotted based on three hypothetical business cases, which form the foundation of each company's proposal to the SPO. Both the companies and their business cases are hypothetical and used solely to illustrate the method.

- Company 1: employs the fewest sensors (12) around the world. As a smaller company the business case is to limit the number of sites and sensors and use standard hardware, offsetting higher costs for using its lower-quality standard sensor by offering more expensive but exquisite capabilities in high-interest locations. It employs mostly 0.3 m telescopes ($1M) while the 0.6 m Teide (Canary Islands), 0.6 m El Leoncito (South America) and 0.8 m Perth (Australia) telescopes cost $1.5M, $1.5M, and $2M respectively. A discount of $0.2M is awarded if either all three large telescopes or all telescopes in the network are picked.
- Company 2: employs the second-most sensors (21) around the world, mixing 0.3 m and 0.4 m telescopes with different FOVs. The business case is to charge more for the 0.4 m ($0.75M) than the 0.3 m ($0.50M) as well as $0.25M extra for any site in the southern hemisphere.
- Company 3: employs the greatest number of sensors (23). The business case is to charge a low cost for its standard sensor (0.40 m, $0.50M) but charge more for its locations in Mt Zin (Israel) and India; one in India is a 0.6 m telescope. An additional $0.20M is added if multiple sensors are used at one site to cover operating costs.

All commercial sensors are based on real-world components. Ackermann's tradestudy for WFOV sensors is used as a foundation to conduct market research on available telescope and camera combinations for NFOV sensors [46]. Lists of telescopes between 0.3 to 0.8 m and appropriate cameras were generated. All possible combinations were compared to determine telescopes which meet the aperture constraint and had a FOV between 0.5°x0.5° and 1.5°x1.5° with a plate scale on the order of 1 arcsec/pixel. The sensors were then placed according to company business cases.

Civil Sensors

The sole US civil sensor represented in this architecture is based on MCAT, NASA's 1.3 m all-regime debris-monitoring telescope on Ascension Island which has already been proposed as a potential contributor to the SSN.

Scientific Sensors

The sole allied scientific sensor is a hypothetical sensor dubbed BIGGO. The sensor is a 2 m, 4°x4° WFOV staring sensor dedicated to astronomical research. This sensor was placed in Brazil after research found a limited SDA presence in this portion of the southern hemisphere.

Summary of Sensor Parameters

Fig. 3 maps all sites in this scenario. Literature review identified open-source specifications for GEODSS and MCAT. Table 1 lists the owner, site, telescope, location, and atmospheric transmission at zenith used for all sensors. Table 2 lists the parameters for each telescope/camera combination employed in the problem. All quantum efficiencies η were pulled for 625 nm and the name Officina Stellare Riccardi (OSR) has been abbreviated.

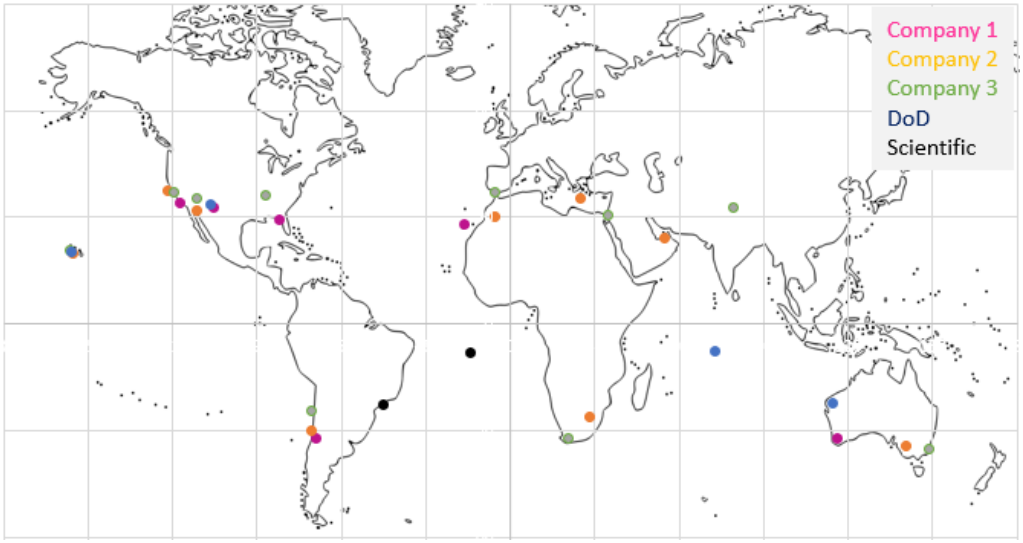

Fig. 3. Map of sites used in study; owners are color-coded.

Table 1. Owner, site, telescope, location, and atmospheric transmission for all sensors.

Network	Site	Sensor #			Lat	Long	$T_{atm,zen}$
		1	2	3			
Company 1	El Leoncito	A			-31.8	-69.3	0.72
Company 1	New Mexico Skies	B	B	B	32.9	-105.53	0.71
Company 1	Perth	C			-32.01	116.14	0.63
Company 1	Rosemary Hill	B	B	B	29.4	-82.59	0.63
Company 1	Table Mtn	B	B	B	34.38	-117.68	0.71
Company 1	Teide	A			28.3	-16.51	0.72
Company 2	Al Sadeem	B	B	B	24.18	54.68	0.63
Company 2	Cerro Tololo	B	B		-30.17	-70.81	0.71
Company 2	Johannesburg	B	B	B	-26.18	28.07	0.69
Company 2	Kitt Peak	B	B		31.96	-111.6	0.7
Company 2	Lick	B	B		37.34	-121.64	0.66
Company 2	Mauna Kea	B	B		19.82	-155.47	0.93
Company 2	Riverland	B	B	B	-34.28	140.37	0.63
Company 2	SaharaSky	B	B		30.24	-5.61	0.64
Company 2	Skinakas	B	D		35.21	24.9	0.69
Company 3	Cerro Paranal	E	F		-24.63	-70.4	0.91
Company 3	Dyer	E	F		36.05	-86.81	0.63
Company 3	Haleakala	E	F		20.71	-156.26	0.75
Company 3	Indian Astro	G	E	F	32.78	78.96	0.95
Company 3	Lowell	E	F		35.2	-111.67	0.71
Company 3	Moron	E	F		37.15	-5.59	0.63
Company 3	Mt Stromlo	E	F	F	-35.32	149.01	0.64
Company 3	Mt Zin	E	F		30.6	34.76	0.64
Company 3	SAAO	E	F		-32.38	20.81	0.69
Company 3	Sierra	E	F	E	37.07	-119.41	0.67
Scientific	Pico dos Dias	H			-22.53	-45.58	0.69
Civil	Ascension	I			-7.97	-14.4	0.63
DoD	Diego Garcia	J	J	J	-7.41	72.45	0.92
DoD	Haleakala (DoD)	J	J	J	20.71	-156.26	0.91
DoD	Socorro	J	J	J	33.82	-106.66	0.79

Table 2. Telescope specifications.

Opt	Telescope & Camera	Dia (m)	FOV (°x°)	Focal Len (m)	f/#	Plate Scale	Pixels	Pitch (um)	η_{625}	e_d	e_r
A	OSR Large Astrograph 600 F3.8 w/FLI ML09000	0.6	0.92x0.92	2.28	f/3.8	1.1	3056x3056	12	0.65	0.03	16
B	Takahashi FET-300 w/FLI ML09000	0.3	0.88x0.88	2.4	f/8	1	3056x3056	12	0.65	0.03	16
C	OSR Large Astrograph 800 F5 w/Apogee ALTA F4320	0.8	0.7x0.7	4	f/5	1.2	2048x2048	24	0.67	2	12
D	Astro Systeme Austria Astrograph 16N Reduced w/FLI ML09000	0.4	1.38x1.38	1.52	f/2.8	1.6	3056x3056	12	0.65	0.03	16
E	Takahashi C-400 w/Apogee ALTA F4320	0.4	0.5x0.5	5.6	f/14	0.9	2048x2048	24	0.67	2	12
F	Astro Systeme Austria Astrograph 16N Reduced w/FLI ML16803	0.4	1.39x1.39	1.52	f/2.8	1.2	4096x4096	9	0.52	0.01	15
G	OSR Large Astrograph 600 F5 w/Apogee ALTA F4320	0.6	0.94x0.94	3	f/5	1.7	2048x2048	24	0.67	2	12
H	Pico Dos Dias w/Spectral Instruments	2	0.63x0.63	5.6	f/2.8	0.6	4096x4096	15	0.65	6	12
I	MCAT w/Spectral Instruments Ascension	1.3	0.68x0.68	5.2	f/4	0.6	4096x4096	15	0.65	6	12
J	GEODSS w/Sarnoff MIT/LL CCID-16	1	1.25x1.64	2.15	f/2.15	2.3	1960x2560	24	0.65	6	12

TRANSLATE NEEDS INTO MEASURES

Moomey's end-to-end system engineering approach for the development of a COTS small telescope architecture combined with AFSPCI 10-610 MUA criteria and Daw & Hejduk's SSN measures were used to guide thought towards potential AN needs, requirements, and measures[7]. Stern & Wachtel's measures in related research were also considered. The following three measures are used to evaluate the high-level performance of AN architectures.

Coverage represents the network's ability to view RSOs in some manner. This many include a simple count of unique RSOs, a tally of important longitudes covered, or account for redundancy in sky area. The simplest measure, which is the number of unique RSOs observed out of the entire number of simulated RSOs, is adopted.

Capacity represents the network's ability to obtain a large number of observations on each RSO. *Average capacity* may be easily represented by getting the number of observations on each RSO, and taking the average of these values.

Latency represents the network's ability to ensure a reasonable time between observations on each RSO. Ideally, the maximum time between successive observations for any RSO should be small. *Average latency* may be represented by calculating the maximum time between observations for each RSO, then taking the average.

Previous work found that calculation of these measures resulted in a very small distribution in coverage. Therefore, in this study the three measures were further broken out by RSO category, where RSOs are prioritized in a 1-5 list for the scheduling routine, and weights applied to category contributions before summing all values. The following equations represent the final formulation:

$$
\begin{aligned}
c &= \sum_{i=1}^{5} w_i \left[\left(\frac{r_i}{R_i} \right) 100 \right] \\
\bar{p} &= \sum_{i=1}^{5} w_i \left[\frac{1}{r_i} \sum_{n_i}^{r_i} o_{n_i} \right] \\
\bar{l} &= \sum_{i=1}^{5} w_i \left[\frac{1}{r_i} \sum_{n_i}^{r_i} \max \left(\{ \Delta t_p \dots \Delta t_q \} \right)_{n_i} \right] \\
w_i &= \{1\ , 0.8, 0.6, 0.4, 0.2\}
\end{aligned}
\tag{1.17}
$$

[7] The hypothetical requirements matrix was omitted from this study for brevity.

where c is the Category-Weighted (CW) Coverage, $\bar{p}$ is the Category-Weighted Average (CWA) Capacity (number of observations/RSO), $\bar{l}$ is the CWA Latency (min), w_i is the weight applied to the category, i is the RSO's category, r_i is the number of unique RSOs in the category, R_i is the total number of RSOs simulated in the category, n_i is the n_{th} RSO in the category, o_{n_i} is the number of observations on the n_{th} RSO in the category, Δt_p is the time between the first two observations, and Δt_q is the time between the last two observations.

DEVELOP MODEL AND SIMULATION

An AN architecture is comprised of the nine GEODSS sensors, MCAT, BIGGO, and any permutation of the 56 sensors offered by the three commercial companies. The selection of any commercial sensor may be represented by a binary choice, and for 56 total sensors there are $2^{56} = 7.2 \text{ x } 10^{16}$ conceivable permutations. Since non-commercial contributions will always be considered in the AN, the number of possible AN architectures requiring evaluation is thus $7.2 \text{ x } 10^{16}$. Reduction of this problem space is addressed via the optimization routine, which evaluated several architectures using the following M&S. Architecture performance in the optical collection of GEO RSOs during a 24-hour scenario on Summer Solstice is assessed using the previously-derived measures. The M&S is conducted using a combination of Systems Tool Kit (STK) and custom routines in Python.

RSO Model

The Space-Track.org Geosynchronous TLE Report for 7 Mar 2020 was pulled which finds 954 unique RSOs. The RSOs are assigned to a Category 1-5 prioritization based in proportion to percentages provided by 18 Space Control Squadron (SPCS) for related work [22]. Data from Celestrak is used to determine which RSOs constitute debris. Lastly, Standard M_v data for each RSO was culled from Calsky. The TLEs are imported into an STK scenario and propagated for the 24-hour period starting on 21 Jun 2019. RSO locations are simulated by propagating in STK while physical parameters are calculated later in Python.

Site Model

All sites are loaded in the STK scenario as facilities at the appropriate latitude/longitude and set to operate at ground level. Each site is constrained to operate only in umbra and track RSOs with elevation $\geq 20°$, solar exclusion angle of 40°, and a lunar exclusion angle of 10°. All other physics parameters, including sensors at each site are modeled later in Python. Each site's extinction coefficient, background radiance, and atmospheric transmission are assumed based on values in literature[8]. A constant extinction coefficient of 0.25 is assumed per Frueh [47]. A constant background radiance of 21 M_v/arcsec^2 is used for clear, cloudless conditions at site zenith per an assumption by Colombi et al. [41]. $T_{atm,zen}$ values calculated by Colombi et al. using high-fidelity modeling for sites common to this study are adopted. Values for all other sites are interpolated using Shell's reporting at 625 nm for an acceptable site at 2000' altitude and a pristine site at 10,000' altitude. Cloud contributions are neglected for this study and all sites are assumed to operate on a cloudless night.

SIMULATE SITE-RSO ACCESSES

All possible site-RSO viewing opportunities, or accesses, and associated data between all 30 sites and 954 RSOs during the 24 hour period is generated using custom STK reports. This data is ultimately fused with sensor and RSO physical parameters via Python to determine physically-realistic collection opportunities for a scheduling routine. The reports include: site-RSO access window times; azimuth, elevation, range, and sun-RSO-earth phase angle during all site-RSO accesses; and angles or vectors to calculate sky and lunar position through the simulation. An assumption is made that 30 s is required to collect two to three streaks on an RSO, slew, and settle each telescope for a sequential collection. This permits the scheduling problem to be discretized into 2,880 possible scheduling opportunities at each sensor, which allows all reporting to be conducted in 30 s intervals. For this study, any scheduled sensor-RSO pair is simply assumed to be successfully collected without any attempt to simulate streak data nor perform OD based on observations.

[8] Future works aspires to use the higher-fidelity LEEDR software package to derive these values.

RSO-Sensor Optical Collection Model and Simulation

The list of 30 s site-RSO accesses is culled per site, and duplicated by the number of sensors at each site to generate a list of possible sensor-RSO accesses. Using the equations in the Optical Collection section and the physical parameters for each RSO, site, and sensor, Python and its Pandas database routine is employed to calculate the SNR for all accesses. Only those meeting the SNR ≥ 6 threshold are advanced to the scheduler.

IMPLEMENT SCHEDULING ROUTINE

Minimizing the uncertainty in an RSO's position knowledge is furthered by collecting observations at different locations along the orbit. This is achievable by developing a scheduling routine which collects on individual RSOs at a dispersion of geographic locations and times. Care is also given to collect RSOs based on their importance while not overly favoring higher-ranked RSOs, ensuring RSOs with fewer collection opportunities are not superseded by those with more opportunities, and maintaining a reasonably current ELSET. Fast computational speed is also desirable. A centralized-tasking, centralized-scheduling algorithm was developed using these requirements. The GEODSS and commercial sites are scheduled together, while MCAT is scheduled using a different but similar scheduler. BIGGO's task list is discussed later.

DoD/Commercial Network Scheduler

Prior to commencing the routine, the RSOs are ordered in the following manner. Through analysis of the underlying Standard M_v data, around 20 RSOs were found to be extremely dim. These RSOs are sorted by number of accesses and added to the list. Through analysis of the underlying TLE data, around 20 RSOs were found to have very old ELSETs. These RSOs are sorted by number of accesses and added to the list. Lastly, the remaining RSOs are grouped by category. Within each category, RSOs are sorted by the number of accesses and added to the list. Sorting RSOs by the number of accesses prioritizes RSOs which are dim and/or geometrically challenging to collect.

When the routine commences, the database of sensor-RSO accesses with SNR ≥ 6 is loaded into Pandas, and the list of RSOs is iterated until no RSOs are left to schedule. The database is queried for each RSO, and around 20 total observations are scheduled at a time. The 20 observations are allocated proportionally to all sites capable of collecting on the RSO so that geographic dispersion is always guaranteed. The observations allocated to each site are then randomly assigned to timeslots on the sensors present at the site. Whenever sensor-RSO accesses are scheduled, the corresponding sensor-time combination is removed from the database so another RSO cannot be scheduled on top of it. Anytime a database query returns no accesses for an RSO, the RSO is removed in the next iteration.

The loop over RSOs continues to schedule in batches of 20 observations per RSO at a time until no accesses remain. Scheduling only 20 observations at a time using the RSO list achieves the goals of prioritized collections without diminishing collections on seldom-accessible and lower-priority RSOs. The routine as-written requires approximately two hours when scheduling the nine GEODSS and 56 commercial sensors against all 954 GEO RSOs as run on a dual-core[9] 2.5 GHz 2nd Generation Intel i5 processor with 8 Gb RAM.

MCAT Scheduler

MCAT's scheduler is adapted from the previous scheduler with the following assumptions. Because MCAT performs a variety of debris-monitoring tasks in multiple orbital regimes, only the first and last hour of possible collections is assumed dedicated to GEO RSO observing. Collections are ordered by number of accesses on debris RSOs. MCAT also chooses to track active satellites as a courtesy to the community and disseminate those observations to DoD. These are prioritized after the debris RSO list and similarly ordered by accesses. Each hour is scheduled separately. The resulting operation successfully schedules 136 RSOs on two separate hours.

BIGGO Scheduling

Scheduling BIGGO is not possible because it is a staring sensor. Instead, it is assumed to point at a fixed Azimuth/Elevation (Az/El) for the entire scenario performing an astronomical mission. Any RSOs passing within +/- 2° of this Az/El combination is assumed to be serendipitously collected. Four separate RSOs are detected over long

[9] Since Python does not by design use multi-processing, all reporting in this study more accurately reflects that of a single core. However, the multiprocessing library can be used to employ additional cores on parallelized portions.

periods during the night. In lieu of reporting all possible collections, only the first and last opportunities for each RSO are returned to DoD for a total of 8 observations.

FIND OPTIMAL ARCHITECTURES

Ideally, the performance of all 7.2×10^{16} architectures would be compared to find the global best architecture. Time and computational expense prohibit this, so the NSGA-II optimization routine is used to advance higher-performing algorithms in a heuristic manner. After multiple trials, a small list of architectures is identified which give the decision-maker purchase options.

Since the 56 commercial sensors are the only variable sensors in AN, the choice may be represented by a 56-bit chromosome where each bit represents using or not using a particular sensor. Each architecture therefore includes observations from the nine GEODSS sensors, MCAT, BIGGO, and the corresponding commercial sensors. In lieu of running the scheduler for every AN permutation evaluated, MCAT and BIGGO's schedules are combined with a scheduler run for all DoD/Commercial sensors, and any sensors which are not employed by the architecture under consideration are merely dropped from the master schedule in the evaluation. This significantly speeds the computational time.

Python's Inspyred optimization library [48] is utilized to run five NSGA-II trials of 100 architectures over 50 generations each. The population size is based on recommendations in literature while the number of generations was determined after simulations of 20, 50, and 100 generations showed this to be an appropriate number. The routine employs the following pseudo-optimization problem:

$$\begin{gathered}
\text{Maximize } c = Q \sum_{i=1}^{5} w_i \left[\left(\frac{r_i}{R_i}\right) 100\right] \\
\text{Maximize } \bar{p} = Q \sum_{i=1}^{5} w_i \left[\frac{1}{r_i} \sum_{n_i}^{r_i} o_{n_i}\right] \\
\text{Minimize } \bar{l} = Q \sum_{i=1}^{5} w_i \left[\frac{1}{r_i} \sum_{n_i}^{r_i} \max\left(\{\Delta t_p \ldots \Delta t_q\}\right)_{n_i}\right] \\
w_i = \{1\ , 0.8, 0.6, 0.4, 0.2\} \\
Q = \begin{cases} 1 & if\ cost \leq \$25M \\ large\ penality & otherwise \end{cases}
\end{gathered} \tag{1.18}$$

Cost is calculated via a lookup function which maps the architecture's sensors, represented by the chromosome, to the company's proposal. For the first generation in each trial, the costs of randomly-selected architectures are evaluated and the routine advances when 100 feasible architectures are available. In all other generations, cost is evaluated first and if it exceeds the constraint the optimality criteria are replaced with an unfavorably large penalty which discourages NSGA-II from advancing that architecture. For feasible architectures, Pandas queries are used to calculate the above measures which are employed as optimality criteria. One NSGA-II trial completes in 30 min on the aforementioned hardware.

4. ANALYSIS AND RESULTS

ARCHITECTURE RESULTS

25,000 architectures were evaluated, of which only around 40% were feasible due to architectures exceeding the $25M cost constraint. Each trial identified several distinct non-dominated architectures. The CW coverage metric was found to have a very small distribution between 297-299, and was typically near 299 for the non-dominated solutions. Therefore, CW coverage was taken as constant which allowed a two-dimensional scatterplot of CWA capacity and CWA latency to reduce the presentation of this analysis. Fig. 4 displays the results, where each architecture is color-coded from lowest cost to $25M by a red/yellow/green gradient and all non-dominated values are circled. Each architecture is named based on its position on the graph, proceeding from the southwest to northeast corners in order of increasing CWA latency.

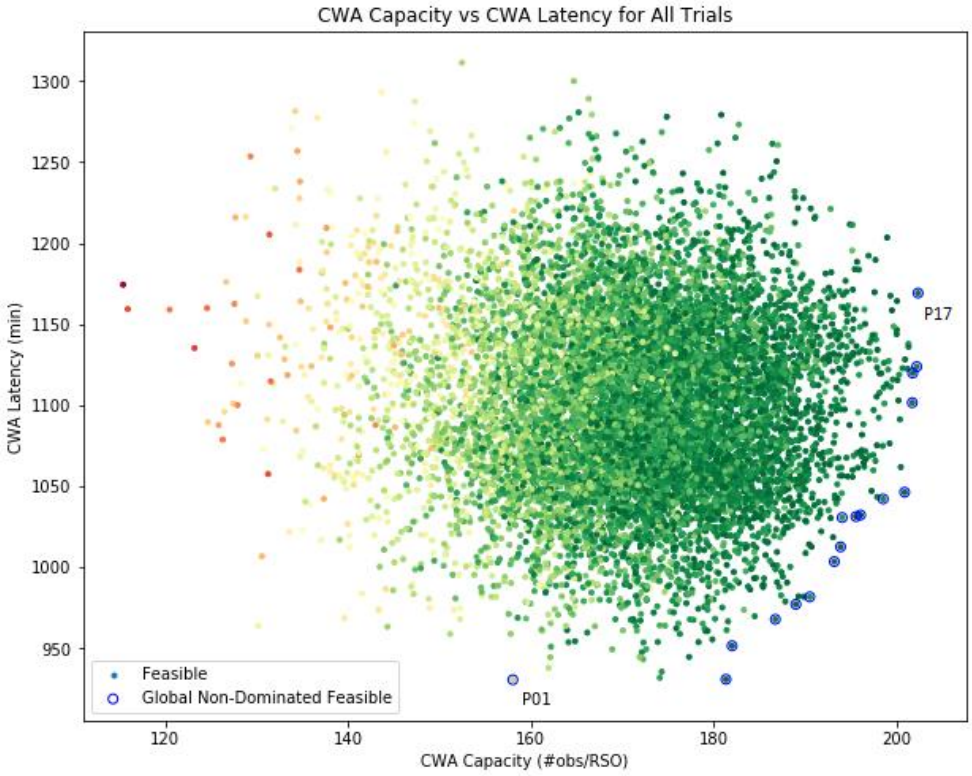

Fig. 4. Feasible architecture CWA Latency vs CWA Capacity, color-coded by architecture cost. Circled values indicate non-dominated architectures, where blue circles indicate global non-dominated solutions.

The graph indicates architectures approaching the Pareto Front are costlier, which is intuitive as adding more sensors improves capability at more cost. Non-dominated values from one trial were found to be dominated by non-dominated values from other trials. Woodruff & Herman's Python Pareto library, implements NSGA-II's non-domination sorting routine [49], was used to further reduce the problem set and identify the 17 global non-dominated architectures. These values are indicated with blue circles and comprise the remainder of this analysis.

The scatterplot generally shows a trade-off between improving CWA capacity and CWA latency. To provide better insight into this trade, the percent error equation is adopted to quantify how far each architecture's measure is from the best possible value. The Percent Unrealized metric is defined as

$$\%\, Unrealized = \frac{|best - achieved|}{best} \text{ x } 100 \tag{1.19}$$

The best CWA capacity and best CWA latency values are used in a calculation for each architecture, which intuitively shows how much the measures deviate from their best possible values. Fig. 5 displays the results.

Percent Unrealized in CWA capacity and non-outlier CWA latency remain below 30% for all architectures. Architectures P03-P08 maintain a 10% difference in both values. An obvious balance exists at the intersection of the blue and yellow lines. Architecture P06 may be thought of as the architecture best approaching the utopia point of the problem.

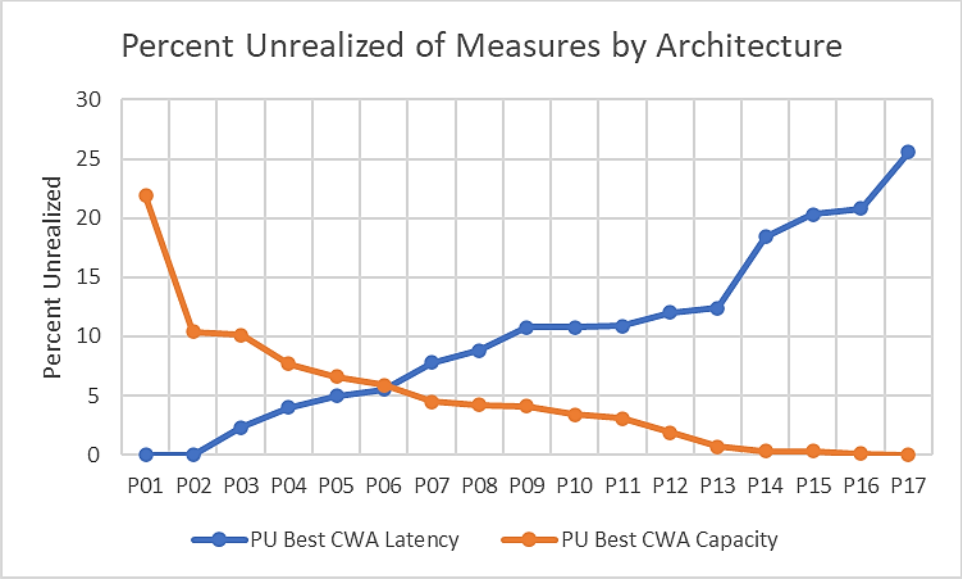

Fig. 5. Percent Unrealized for each architecture. The architectures near the intersection of the yellow and blue lines represents those which best balance the trade between CWA capacity and CWA latency.

Fig. 6 provides summary statistics for the best architectures. The architectures cost $20.6M to $25M, have a CW coverage of 300, CWA capacity of 115 to 202 observations/RSO, a CWA latency of 931 to 1311 minutes, and use 24 to 35 sensors from a mix of companies.

The bottom subplot shows the percent of sensors used from each company out of all sensors in the architecture on the primary axis and the total number of sensors used on the secondary axis. For example, Architecture P01 uses 24 sensors, 46% of which come from Company 3, 29% from Company 1, and 25% from Company 2. It is seen that most architectures are comprised more of Company 3's sensors and less from Company 1's sensors. This indicates Company 3's capabilities, in general, are key to achieving higher-quality SDA collection. However, it should be noted that Company 3 provides the largest number of sensors in the scenario.

The middle subplot shows each company's percent utilization per architecture, or the number of company sensors in the architecture out of all of the sensors offered by the company. This metric may be important to a decision-maker as it illuminates the usefulness of an offering, as well as how a company's business case may be affected if it receives a very low or very high utilization. Company 3 typically has a high utilization while Companies 1 and 2's utilizations vary throughout the architectures. Architectures P04 and P08 are noteworthy since company sensor utilizations are within 15% of each other and near 50% utilization.

The top subplot shows the monetary amount awarded to each company on the primary axis and the total architecture cost on the secondary axis. There are several architectures under the $25M cost threshold, with Architecture P01 having the lowest cost. Amongst the choices, Company 3 generally stands to make the most profit while Company 1 and Company 2 alternate in second place. However, amongst the architectures there is a noticeable spread in the amount awarded to each company. In contracting scenarios where it is appropriate and desirable to spread awards evenly, Architectures P08, P04, and P06 may be looked upon more favorably.

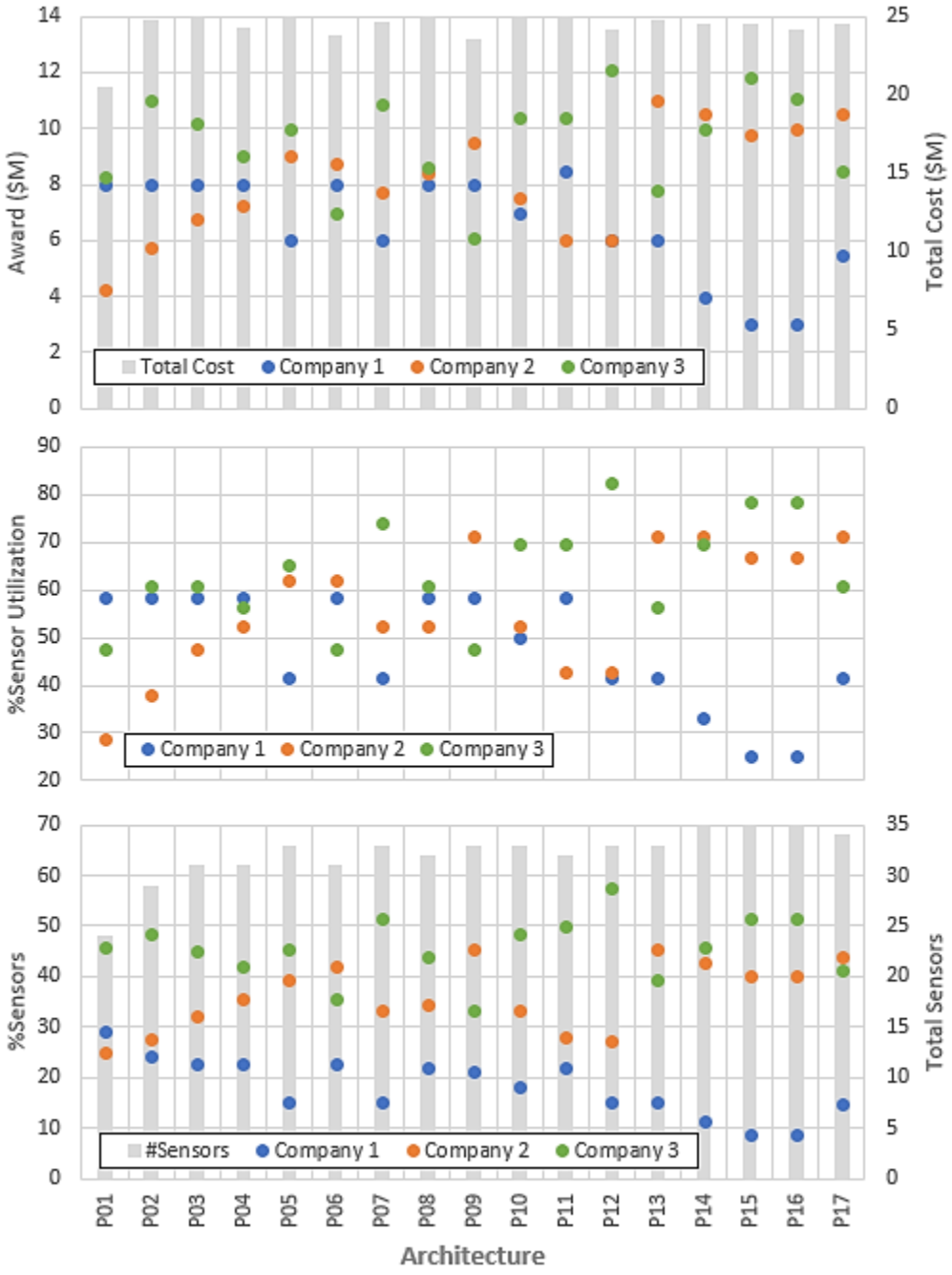

Fig. 6. Comparison of percent of sensors used per company, percent sensor utilization per company, and award to each company per architecture. Company 3 dominates in percent of sensors used while Company 1 and Company 3 tend to have higher sensor utilization. The amount and distribution of awards is variable.

Table 3 depicts the sensors used in each global non-dominated architecture, where the bottom rows shows the percent of all global non-dominated architectures using each particular sensor and the diameters of the sensors. Both rows are independently color-coded using a red/yellow/green gradient with a higher percent of architectures and larger diameter colored green, respectively. Two of Company 1's twelve sensors, five of Company 2's 21 sensors, and twelve of Company 3's 23 sensors respectively are used in 70% or more of all architectures. Notably, 94% of all architectures used sensors at Kitt Peak, Mauna Kea, the South African Astronomical Observatory (SAAO), and the Sierra Nevada site. Conversely, all companies hosted sites which were chosen in less than 25% of the optimal

architectures. Notably, Company 1's site at Teide in the Canary Islands was not present amongst any of the optimal architectures.

Using aperture diameter as a proxy for sensor performance, it can be seen that larger aperture does not necessarily correlate to higher selection amongst the global non-dominated architectures. In fact, of the four large commercial aperture telescopes used in the simulation only one, the 80 cm telescope in Perth Australia, was chosen in a majority of architectures. Other factors such as location, cost, and the number and brightness of RSOs in the viewing area all contribute to the calculate of measures. It is noted that use of a heuristic method such as NSGA-II to cull only a handful of the possible architectures, with a further reduction to illuminate only the optimal performers, prohibits sweeping conclusions about the entire dataset to be made.

Table 3. Sensor employment and percent of global non-dominated architectures using each sensor

	Company 1											
Arch	El Leoncito1	New Mexico Skies1	New Mexico Skies2	New Mexico Skies3	Perth1	Rosemary Hill1	Rosemary Hill2	Rosemary Hill3	Table Mtn1	Table Mtn2	Table Mtn3	Teide1
P01		X	X	X	X		X			X	X	
P02		X	X	X	X		X			X	X	
P03		X			X	X	X	X	X		X	
P04			X	X	X		X	X	X		X	
P05		X		X	X		X	X				
P06		X		X	X			X	X	X	X	
P07		X	X		X		X	X				
P08		X	X		X	X	X		X	X		
P09			X	X	X	X	X			X	X	
P10			X	X	X	X		X	X			
P11	X		X	X	X			X	X	X		
P12				X	X		X		X		X	
P13		X		X	X				X		X	
P14				X		X			X		X	
P15			X						X	X		
P16			X						X	X		
P17	X	X		X		X					X	
%archs using	12	53	59	71	76	35	53	41	65	47	59	0
dia (cm)	60	30	30	30	80	30	30	30	30	30	30	60

	Company 2																				
Arch	Al Sadeem1	Al Sadeem2	Al Sadeem3	Cerro Tololo1	Cerro Tololo2	Johannesburg1	Johannesburg2	Johannesburg3	Kitt Peak1	Kitt Peak2	Lick1	Lick2	Mauna Kea1	Mauna Kea2	Riverland1	Riverland2	Riverland3	SaharaSky1	SaharaSky2	Skinakas1	Skinakas2
P01								X	X	X			X			X	X				
P02							X	X	X	X	X	X	X				X				
P03							X	X	X	X		X	X	X					X	X	X
P04			X			X			X		X	X	X	X			X	X	X	X	
P05	X					X	X	X	X	X	X	X			X	X		X	X		X
P06			X				X	X	X	X	X	X	X	X	X			X		X	X
P07		X					X	X	X		X	X	X		X	X	X			X	
P08					X	X	X		X	X		X	X	X			X	X			X
P09	X	X	X					X	X	X	X	X	X	X	X			X	X	X	X
P10		X				X	X	X	X	X			X		X			X	X	X	
P11					X			X	X		X	X	X	X	X				X		
P12	X			X			X			X	X	X	X			X		X			
P13	X	X	X		X	X	X		X			X	X	X	X	X	X	X		X	
P14		X	X	X			X		X		X	X	X	X	X	X	X	X		X	X
P15	X	X	X		X	X	X		X				X	X	X	X		X	X	X	
P16	X	X	X		X	X	X		X				X	X		X	X	X	X	X	
P17	X	X		X	X	X	X		X	X		X	X	X				X	X	X	X
%archs using	41	47	41	18	35	47	76	53	94	59	53	76	94	65	53	47	47	71	53	65	41
dia (cm)	30	40	40	30	40	40	40	30	30	40	30	40	30	40	30	30	40	30	30	30	40

	Company 3																						
Arch	Cerro Paranal1	Cerro Paranal2	Dyer1	Dyer2	Haleakala1	Haleakala2	Indian Astro1	Indian Astro2	Indian Astro3	Lowell1	Lowell2	Moron1	Moron2	Mt Stromlo1	Mt Stromlo2	Mt Stromlo3	Mt Zin1	Mt Zin2	SAAO1	SAAO2	Sierra1	Sierra2	Sierra3
P01						X	X		X	X			X	X		X			X	X	X		X
P02					X	X	X	X	X	X			X		X	X		X	X	X	X		X
P03					X	X		X	X		X	X	X	X			X	X	X	X		X	X
P04						X			X	X	X	X			X	X	X	X	X	X	X		X
P05			X	X		X		X	X		X		X	X	X	X		X		X	X	X	X
P06			X	X	X	X					X				X	X		X		X	X		X
P07			X	X	X	X			X	X	X	X	X	X	X	X		X	X		X	X	X
P08		X	X	X	X			X		X	X			X	X	X				X	X	X	X
P09	X				X					X			X	X	X	X			X	X	X		X
P10	X		X	X	X	X			X	X	X	X		X		X		X	X	X	X		X
P11	X		X	X	X	X		X	X	X				X	X	X			X	X	X	X	X
P12	X	X	X	X	X	X			X	X	X	X		X	X	X	X		X	X	X	X	X
P13	X	X		X		X			X	X	X				X				X	X	X	X	X
P14	X	X			X				X	X	X	X		X	X	X	X		X	X	X	X	X
P15	X	X	X	X	X	X		X	X	X	X	X		X	X				X	X	X	X	X
P16	X	X	X	X	X	X			X	X	X	X		X	X	X			X	X	X	X	X
P17	X	X		X	X	X				X		X	X	X				X	X	X	X	X	
%archs using	53	41	53	65	76	82	12	35	76	82	71	53	41	76	76	76	24	47	82	94	94	65	94
dia (cm)	40	40	40	40	40	40	60	40	40	40	40	40	40	40	40	40	40	40	40	40	40	40	40

QUANTIFYING UTILITY OF CIVIL AND SCIENTIFIC SENSOR DATA

Although the preceding analysis emphasized the contributions of commercial sensors, the underlying data also includes the observations from civil and scientific sensors. One way to assess the contributions of these sensors is to compare AN measures as calculated both with and without these sensors' contributions. Review of the data shows including the additional observations only improved CW coverage by 0.1%. However, in true numbers this translates into 1-3 unique RSOs provided to the AN by the contributing sensors. CWA capacity was generally improved by 0.3% when the extra data was included. Interestingly, inclusion of the additional data increased CWA latency by up to 1%.

Because MCAT and BIGGO contributed limited observations on a small amount of the total RSOs simulated in this scenario, reporting on only these RSOs provides insight. Including the additional data improved the capacity of these RSOs by 3-5%. However, latency was again increased by up to 5%.

Latency increasing when additional observations on RSOs are taken seems counter-intuitive. One possible explanation in this scenario is the fact that most of the contributing observations were from MCAT, which collects only during the beginning and end of its viewable period. If the collection times on these RSOs by other sensors is far from these times, naturally a longer maximum time between observations will be calculated once MCAT's observations are included which will roll up into a higher average AN latency. Adding any unique RSOs by the contributing sensors may have a similar effect—new RSOs will have fewer observations, possibly spaced further in time, which ultimately raises the latency calculation. Further investigation is required, which may necessitate rethinking the latency measure.

INTERMEDIATE CONCLUSIONS AND RECOMMENDATIONS

It is apparent that Company 3's large number of sensors helped in its selection. Company 1's business case to deploy only a few sensors with high-quality assets in good locations may be tenuous. Although its high-performing asset in Perth is selected in 80% of the architectures, it generally receives the second or third most award in the optimal architectures. Based on the preceding analysis, Table 4 provides the following five recommended architectures for a decision-maker. These architectures consider relative performance, cost, equity in award fee to each company, and

the expected sensor utilization of each company. Architectures P04, P06, and P08 are felt to be ideal selections with similar performance whose distinctions require managerial consideration. Architectures P01 and P17 are proposed as those which maximize one performance measure at the expense of the other and come in under cost by awarding dissimilar amounts to the three companies.

Table 4. Recommendations for SPO decision-maker

Selection	Advantages	Disadvantages
P04	- Near-best balance (<10% best latency, < 5% best capacity) - Fairly similar award ($8/7.3/9M) - Best sensor utilization (58/52/57%) - Under cost ($24.25)	- None
P06	- Best balance (<5% latency and capacity) - Fairly similar award ($8/8.8/7) - Under cost ($23.75)	- Slightly dissimilar sensor utilization (58/62/48%)
P08	- Near-best balance (<10% best latency, < 5% best capacity) - Most similar award ($8/8.5/8.5M) - Good sensor utilization (58/52/61%)	- No cost saving ($25M)
P01	- Best latency - Lowest cost ($20.6M)	- Worst capacity - Dissimilar award ($8/4.3/8.3M)
P17	- Best capacity - Under cost ($24.5M)	- Worst latency - Dissimilar award ($5.5/10.5/8.5M)

5. CONCLUSIONS AND FUTURE WORK

This multi-disciplinary study addressed a method to improve USG SDA cataloging by employing system architecting, physics-based modeling, optimization, and data analysis to determine how to optimally incorporate non-traditional sensors into the SSN. A large tradespace of around 10^{16} architectural choices was smartly evaluated to leave a decision-maker with five courses of action based on a balance of technical performance measures and business factors. The methodology lays a foundation for assessing future AN options. Immediate areas for improvement include reassessing the measures, investigating alternate optimization schemes, and improving the scheduling routine.

This study is part of an ongoing research effort assessing AN cataloging capabilities. Future work will consider the larger deep-space regime, additional ground and space-based sensors, improving the modeling of physical parameters, using covariance uncertainty and other stochastics in the collection scenario, conducting orbital determination during the routine, and simulating on different nights of the year. Therefore several of the obvious limitations of the present work are intended to be addressed in successive studies.

6. ACKNOWLEDGEMENTS

The authors wish to acknowledge use of AGI's STK and STK Connect programs for the orbital aspects of this project. Additionally, this work would not be possible without the efforts made by the developers of Python and the Pandas, Inspyred, and Pareto routines. Last, gratitude is extended to members of the SDA community for their insight and feedback throughout this endeavor.

7. REFERENCES

[1] "Space Situational Awareness Efforts and Planned Budgets," *Government Accountability Office*, 2015.
[2] E. Crawley, B. Cameron, and D. Selva, *System Architecture: Strategy and Product Development for Complex Systems*. Prentice Hall Press, 2015.
[3] E. Rechtin and M. W. Maier, *The Art of Systems Architecting*, 3rd ed. CRC press, 2010.
[4] G. S. Parnell, T. A. Bresnick, S. N. Tani, and E. R. Johnson, *Handbook of Decision Analysis*. John Wiley & Sons, 2013.
[5] K. Deb, *Multi-Objective Optimization Using Evolutionary Algorithms*. John Wiley & Sons, 2008.

[6] K. Y. Lee and M. A. El-Sharkawi, *Modern Heuristic Optimization Techniques: Theory and Applications to Power Systems*. John Wiley & Sons, 2008.
[7] K. Deb, A. Pratap, S. Agarwal, and T. Meyarivan, "A Fast and Elitist Multiobjective Genetic Algorithm: NSGA-II," *IEEE Trans. Evol. Comput.*, vol. 6, no. 2, pp. 182–197, 2002.
[8] R. L. Haupt and S. Ellen Haupt, "Practical Genetic Algorithms," 2004.
[9] C. R. Reeves, "Using Genetic Algorithms with Small Populations," in *Proceedings of the 5th International Conference on Genetic Algorithms*, 1993, vol. 590, p. 92.
[10] "Genetic Algorithm Minimum Population Size." StackExchange.com, 2014.
[11] D. A. Vallado, *Fundamentals of Astrodynamics and Applications*, 4th ed. Microcosm Press, 2013.
[12] M. R. Ackermann, R. R. Kiziah, P. C. Zimmer, and J. T. McGraw, "Weather Considerations for Ground-Based Optical Space Situational Awareness Site Selection," in *Advanced Maui Optical Surveillance Conference*, 2018.
[13] J. R. Shell, "Optimizing Orbital Debris Monitoring with Optical Telescopes," in *Advanced Maui Optical Surveillance Conference*, 2010.
[14] S. B. Howell, *Handbook of CCD Astronomy*, 2nd ed. Cambridge University Press, 2006.
[15] G. M. Thomas and R. G. Cobb, "Ground-based, Daytime Modeling and Observations in SWIR for Satellite Custody," in *Advanced Maui Optical Surveillance Conference*, 2019.
[16] M. M. Schmunk, "Initial Determination of Low Earth Orbits Using Commercial Telescopes," Master's Thesis, Air Force Institute of Technology, 2008.
[17] K. Krisciunas and B. E. Schaefer, "A Model of the Brightness of Moonlight," *Publ. Astron. Soc. Pacific*, vol. 103, no. 667, p. 1033, 1991.
[18] B. Tapley, B. Schutz, and G. H. Born, *Statistical Orbit Determination*. Elsevier, 2004.
[19] R. R. Bate, D. D. Mueller, and J. E. White, *Fundamentals of Astrodynamics*. Dover Publications, 1971.
[20] United States Strategic Command, "Strategic Command Directive 505-1, Space Surveillance Operations—Basic Operations, Volume 1." 2004.
[21] A. B. Poore *et al.*, "Covariance and Uncertainty Realism in Space Surveillance and Tracking," 2016.
[22] K. Dararutana, "Comparison of Novel Heuristic and Integer Programming Schedulers for the USAF Space Surveillance Network," Master's Thesis, Air Force Institute of Technology, 2019.
[23] National Research Council, "Continuing Kepler's Quest: Assessing Air Force Space Command's Astrodynamics Standards," 2012.
[24] T. Chow, "Space Situational Awareness Sharing Program: An SWF Issue Brief," *Secure World Foundation, Washington, DC*, 2011.
[25] D. J. Trump, "Space Policy Directive 3, National Space Traffic Management Policy." Jun 2018.
[26] B. L. Wilson, "Space Surveillance Network Automated Tasker," *Adv. Astronaut. Sci.*, vol. 119, no. Part 1, pp. 377–386, 2004.
[27] B. Lal, A. Balakrishnan, B. M. Caldwell, R. S. Buenconsejo, and S. Carioscia, "Global Trends in Space Situational Awareness (SSA) and Space Traffic Management (STM)," Science and Technology Policy Institute, 2018.
[28] Office of the United States Air Force Chief Scientist, "Technology Horizons: A Vision for Air Force Science and Technology 2010-30," 2011.
[29] The White House, "National Security Strategy," 2017.
[30] B. Houlton and D. Oltrogge, "Commercial Space Operations Center (ComSpOC): A Commercial Alternative for Space Situational Awareness (SSA)," in *30th Space Symposium Technical Track*, 2014.
[31] B. R. Flewelling, B. Lane, D. L. Hendrix, W. Therien, and M. W. Jefferies, "Recent Events and Highlights in Space Situational Awareness: Exploitation of Global Persistent, Real-Time Optical Observations of Deep Space," in *34st Space Symposium*, 2018.
[32] J. Aristoff and N. Dhingra, "Non-Traditional Data Collection and Exploitation for Improved GEO SSA via a Global Network of Heterogeneous Sensors," in *Advanced Maui Optical Surveillance Conference*, 2018.
[33] Orbital Debris Program Office, "Optical Measurements." . NASA.gov.
[34] S. M. Lederer *et al.*, "The NASA Meter Class Autonomous Telescope: Ascension Island," 2013.
[35] C. T. Bellows, "Leveraging External Sensor Data for Enhanced Space Situational Awareness," PhD Dissertation, Air Force Institute of Technology, 2015.
[36] Wikipedia, "Extremely Large Telescope." .
[37] Wikipedia, "List of Largest Optical Reflecting Telescopes." .
[38] D. Moomey, "A Call to Action: Aid Geostationary Space Situational Awareness with Commercial Telescopes," *Air & Space Power Journal*, vol. 29, no. 6, pp. 12–31, 2015.

[39] J. Raley, R. Weisman, C. Chow, M. Czajkowski, and K. Sotzen, "OrbitOutlook: Autonomous Verification and Validation of Non-Traditional Data for Improved Space Situational Awareness," in *Advanced Maui Optical Surveillance Conference*, 2016.
[40] M. R. Ackermann, D. D. Cox, R. R. Kiziah, P. C. Zimmer, J. T. McGraw, and D. D. Cox, "A Systematic Examination of Ground-Based and Space-Based Approaches to Optical Detection and Tracking of Artificial Satellites.," in *30th Space Symposium Technical Track*, 2015.
[41] J. M. Colombi, J. L. Stern, S. T. Wachtel, D. W. Meyer, and R. G. Cobb, "Multi-Objective Parallel Optimization of Geosynchronous Space Situational Awareness Architectures," *Journal of Spacecraft & Rockets*, pp. 1–13, 2018.
[42] M. G. Bateman, J. M. Colombi, R. G. Cobb, and D. W. Meyer, "Exploring Alternatives for Geosynchronous Orbit Space Situational Awareness," unpublished paper, Mar 2018.
[43] M. S. Felten, J. M. Colombi, R. G. Cobb, and D. Meyer, "Optimization of Geosynchronous Space Situational Awareness Architectures Using Parallel Computation," in *Advanced Maui Optical Surveillance Conference*, 2018.
[44] R. F. Bruck and R. H. Copley, "GEODSS Present Configuration and Potential," in *Advanced Maui Optical Surveillance Conference*, 2014.
[45] G. North, "A Better Formula for Telescopic Limiting Magnitudes?," *J. Br. Astron. Assoc.*, vol. 107, no. 2, p. 82, 1997.
[46] M. R. Ackermann, P. Zimmer, J. T. McGraw, and E. Kopit, "COTS Options for Low-Cost SSA," in *Advanced Maui Optical Surveillance Conference*, 2015.
[47] C. Frueh and M. K. Jah, "Detection Probability of Earth Orbiting Objects Using Optical Sensors," *Adv. Astronaut. Sci.*, 2013.
[48] Garrett, Aaron Lee, "Inspyred: Bio-inspired Algorithms in Python." 2012.
[49] Woodruff, Matthew J. and Herman, Jon D., "Pareto.py: Nondominated Sorting for Multi-Objective Problems." 2018.